



**IJITCE**

**ISSN 2347- 3657**

# **International Journal of Information Technology & Computer Engineering**

[www.ijitce.com](http://www.ijitce.com)



**Email : [ijitce.editor@gmail.com](mailto:ijitce.editor@gmail.com) or [editor@ijitce.com](mailto:editor@ijitce.com)**

## MPPT FOR HYBRID PHOTOVOLTAIC/WIND/FUEL CELL POWER SYSTEM USING ARTIFICIAL NEURAL NETWORK

Koram Veronica Vinny

Assistant professor

Department Of EEE

NAWAB SHAH ALAM KHAN COLLEGE OF ENGINEERING & TECHNOLOGY

NEW MALAKPET, HYDERABAD-500 024

**Abstract:** Hybrid power systems new energy management approaches are covered in this article. An Artificial Neural Network (ANN) is used in the suggested management system in order to govern the flow of power between the hybrid powersystem to meet the demands of the system. To accomplishmaximumpowerpointtracking(MPPT) from a variety of energy sources, including photovoltaics (PV), wind turbines, fuel cells the neural network controller is used. Hybrid systems with PV panels, wind turbines (WTs), and fuel cells for hybrid system support with DC-DC converters are used to test the developed ANN-based approach. A control strategy is implemented with the ANN controller for smoothing the power fluctuation. Different operating conditions are used to test the proposed model's dynamic behavior. The proposed hybrid system provides more power than PV, WT, and FC systems atdifferentloads,accordingtotheanalysis. Forboth the stand-alone system and the grid, this research can be applied. For PV panels, wind turbines, and Fuel Cells with DC-DC converters for DC loads, the ANN performs better than Fuzzy in the MPPT approach. MATLAB/Simulink is used to simulate the results of the Fuzzy and ANNanalysis.

Keywords:- MPPT, Artificial Neural Network (ANN), Photo Voltaic(PV) cell, Wind Turbine (WT), Fuel Cell, DC link

### I. INTRODUCTION

Renewable energy sources are showing enormous promise as we go into the next decade and toward a greener energy. In terms of renewable energy generation, Solar and wind energy are two of the most promising renewable power generation technologies among these renewable energysources. Eventhemostoptimisticpredictions of the growth of photovoltaic and wind power generation systems were exceeded. Using a renewable energy source in a dynamic way might also cause stability and power quality issues thatare uncommon in conventional power systems. As a result, the management of the hybrid system's energy flow is critical to the membrane's long-term viability and to the continuous flow of energy. In order to spur the development of alternative energy sources, it is essential to overcome this obstacle. Solar photovoltaic (PV) and wind turbine (WT) are two examples of non-conventional energy sources that have been established in the recent decade. Because of their abundance, cleanliness, and cost-effectiveness[1,2] they have become an essentialpart of everyday life. To meet the growing need for power, fuel cells (FC) are also being deployed. There are a few research papers on energy management in hybrid power systems provided in the literature [2]. Wang and Nehrir [3] suggested a DC-linked hybrid wind/PV/FC energy system power management approach. A power management method for a hybrid PV/wind turbine/FC system was given in this study by the author. In [4], Ahmed et al. a hybrid PV/wind/FC power system with an ultra-capacitor bank was studied in detail by Onar et al. [5] and a power management strategy algorithm was created. The fluctuating nature of renewable energy resources power generation from renewable energy systems are intermittent. These circumstances motivated to combine two or more energy sources with storage system to make Hybrid Renewable Energy System [1-3]. An isolated hybrid system gives a higher efficiency with a low cost of energy production, compared to the system with a single source [4].

Conventional approaches to hybrid power system control, such as the linear PI controller (which has been shown to be unstable in the face of a varietyof changes in weather conditions), were utilized in all of the earlier methods. It's a fantastic chance for distributed power generation with the hybrid renewable energy system (HRES). In addition to Wang and Nehrir [3], Ahmed et al. [4] and Onar et al. [5] presented power management strategies for AC-linked hybrid wind/PV/FC energy systems, respectively,whileOnaretal.[5]proposedapower management strategy algorithm for a hybrid PV/wind/FC power system with an ultra-capacitor bank. Wind turbine energy systems are the fastest- growing system innovation in terms of the rate of yearly growth of the introduced limit perinnovation source. ' The best solution for today's innovation is to create a wind turbine energy system [6,7]. It is easy to integrate PV systems with existing DC-DC power converters since they can be scaled from small to large [8-12]. A hierarchical controller between four energy sources, including PV panels, wind turbines, and fuel cells, is introduced in the suggested method. Fig.1 shows a block diagram of the hybrid power system that was created. The

WT and PV have become the most promising interchange wellsprings of energy. Using the MPPT control approach, DC-DC converters can be used to generate stable power from renewable energy sources. Different MPPT strategies for FC systems have been developed, including the Perturb and Observe (P&O) MPPT method, which is widely used because of its simplicity in determining capacity estimates [13, 14]. Research has shown that utilizing artificial intelligence in a hybrid car can control the FC system within a specified high-efficiency range. It follows that this research proposes a novel adaptive management technique for hybrid power systems that utilizes a neural network to control power flow. In this work, use the MPPT control approach to maximize the power of the PV, WT, and FC systems, and integrate all systems at the DC-link to give the hybrid power.

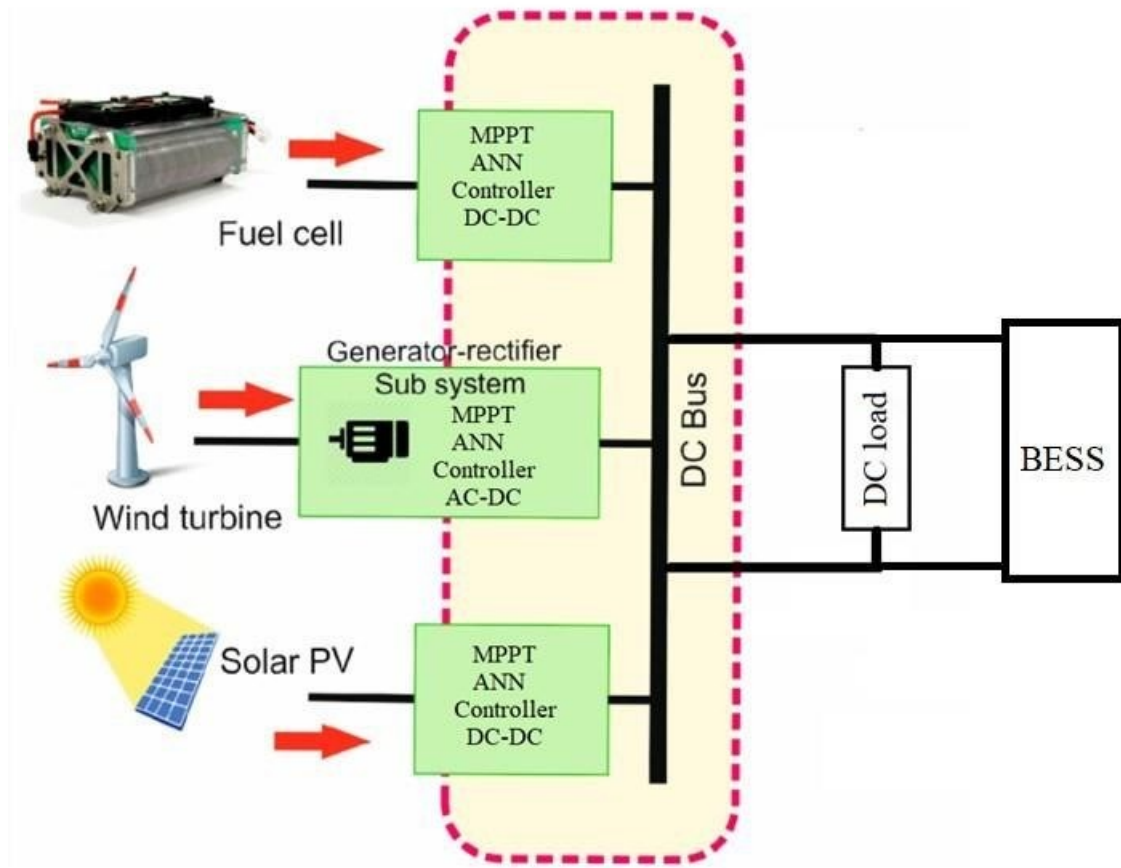


Fig1. Block Diagram of the proposed Hybrid System.

## II. MATHEMATICAL ANALYSIS OF PHOTO-VOLTAIC PV, WIND TURBINE AND FUEL CELL SYSTEMS.

Fig.2 shows the equivalent circuit of a PV cell. In practice, PV cells are combined together into bigger units called PV modules, and these modules are reconnected in series or parallel to create PV arrays, which are used to generate electricity in PV systems. The cell photocurrent is represented by the current source  $I_{ph}$ . Its inherent shunt and series resistances,  $R_{sh}$  and  $R_s$ , are known as the cell's  $R_s$  and  $R_{sh}$  correspondingly. Fig.3 depicts the comparable circuit for a photovoltaic array.

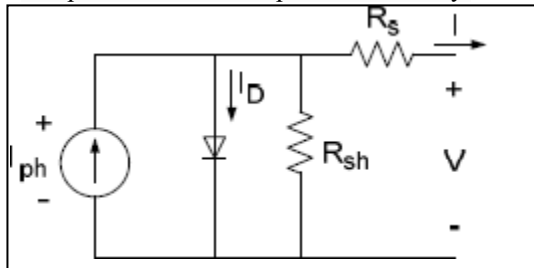


Fig 2. Equivalent circuit of solar array.

Solar cell voltage-current characteristics are given in the form of an equation.

$$I_{ph} = [I_{sc} + K_i(T - 298)] \times I_r / 1000 \quad (1)$$

The photo-current (A) generated by  $I_{ph}$  is shown. At 25 °C and 1000 watts/m<sup>2</sup>, the short-circuit current of a cell is  $I_{sc}$ , and the operating temperature is K. Solar irradiation (W/m<sup>2</sup>):  $I_r$ .

Inverting saturation current ( $I_{rs}$ ) in the module:

$$I_{rs} = I_{sc} / [e^{(\frac{qV_{oc}}{NsKnT})} - 1] \quad (2)$$

Here, q: electron charge, =  $1.6 \times 10^{-19}$  C;  $V_{oc}$ : open circuit voltage (V);  $N_s$ : number of cells connected in series; n: the ideality factor of the diode; k: Boltzmann's constant, =  $1.3805 \times 10^{-23}$  J/K.

With respect to module saturation current  $I_0$ , it is known that:

$$I_0 = I_{rs} \left[ \frac{T}{T_r} \right]^3 e^{\left[ \frac{qEg0}{nk} \left( \frac{1}{T} - \frac{1}{T_r} \right) \right]} \quad (3)$$

$Eg0$ : semiconductor's band gap energy, which is equal to 1.1 eV; PV module's current output is:

$$I = N_p x I_{ph} - N_p x I_0 [e^{\left( \frac{V/N_s + I x R_s/N_p}{n x V_t} \right)} - 1] - I_{sh} \quad (4)$$

With

$$V_t = \frac{k x T}{q} \quad (5)$$

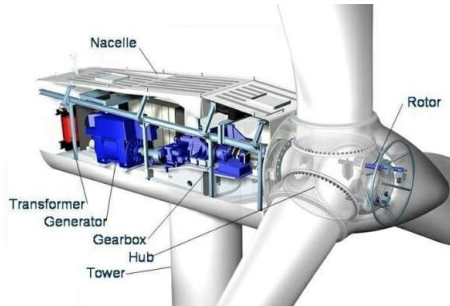
$$I_{sh} = \frac{V x N_p / N_s + I x R_s}{R_{sh}} \quad (6)$$

Here: Number of parallel PV modules ( $N_p$ ) Voltage drop across a diode due to thermal conductivity is called  $V_t$  (V).

### III. Modelling of wind turbines

There are two conversion processes in the wind turbine induction generator (WTIG) system. Mechanical energy must first be transformed into electrical power, and then electrical power must be converted into mechanical energy. The interior pieces of a wind turbine system are shown in cross-section in Fig. 3. A rotor's sharp edges provide WT with the air it needs, which it then trades for power with the axis is point of the rotor. A gearbox is used to raise the generator's shaft's revolutions per minute (rpm). Energy is converted from mechanical to electrical at the shaft attached to the

electrical generator. Whenever the wind condition changes, the power generated is organized into matrices to account for the fluctuation in the conditions. For a final expression of the system's electrical energy, look no further than Eq. (4)



[28], which shows an amazing cubic equation showing the arrangement of internal parts of a wind turbine

$$P_m = \frac{1}{2} C_p (\lambda, \beta) \rho A V^3 \quad (7)$$

$Q$  = air density ( $\text{kg/m}^3$ ),  $A$  = area swept across the rotor blades ( $\text{m}^2$ ),  $k$  = tip-speed ratio,  $V$  = wind speed ( $\text{m/s}$ ),  $b$  is the pitch angle ( $\text{rad}$ ). As a result of aerodynamic rules, the power in the air flow can be converted from one turbine type to another.

As a measure of air flow's power,

$$P_{air} = \frac{1}{2} \rho A V^3 \quad (8)$$

The wind turbine's aerodynamic efficiency is measured by the coefficient function of power,  $C_p$ ;  $k$ , which is given by:

$$C_p = \frac{P_m}{P_w} \quad (9)$$

Wind turbine output ( $C_p$ ) is calculated using  $P_w$  (input power) and  $C_p$  (real power extracted through the wind turbine)( $k$ ).

The blade is twisted away from its longitudinal axis at an angle  $b$ . It's easy to see how  $k$  can be defined as the ratio of rotor speed to wind speed.

$$TSR (\lambda) = \frac{R \omega}{V} \quad (10)$$

The rotor of a wind turbine is referred to as:

$$P_{wt} = C_p \cdot P_{air} \quad (11)$$

$P_{wt}$  = rotor power (W),  $\omega$  = rotor-shaft speed (rad/s), and  $R$  = rotor swept area radius (W) (m). The upper limit for the aerodynamic rotor coefficient in the ideal case of infinite blades and no losses is the Betz limit.  $C_{pmax}$  is equal to 0.593.

Fig 4 depicts a mathematical model of a proton exchange membrane fuel cell (PEMFC). PEM, GDL, CL, GC, and CC of the anode and cathode are all components of the FC, as is the gas diffusion layer (GDL). 3.3.1 Fuel cell equations of physics Species and charge are included in the fundamental fuel cell model. There are five fundamental equations at the core of this paradigm. To define polymer electrolyte reaction kinetics and electro-osmotic drag, equations are connected between electrochemical processes across the source terms. The vector form can be used to specify the equations.

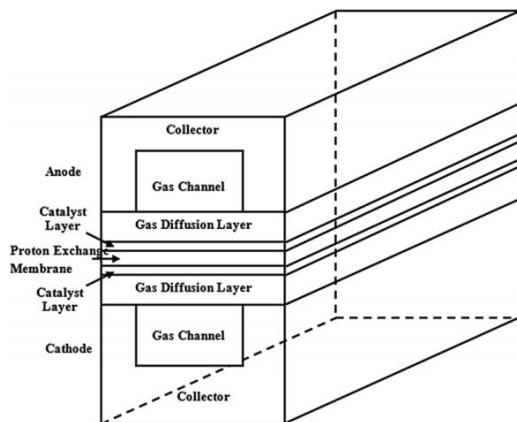


Fig. 4 Model representation of a proton exchange membrane fuel cell.

#### Techniques for maximizing the power of tracking points

The MPPT technique improves the efficiency of WT, solar PV, and FC when they are working together to provide the most power. MPPT can be done in a variety of ways. P&O, INC, the fuzzy logic controller (FLC), and neural network control methods are some of the most widely used approaches for maximizing power point tracking (MPPT). If the output power of the photovoltaic cluster and the underlying rotor speed of the wind turbine are not equal, the two systems are in balance. Under the subject of expanding yield power, the underlying reference values have to be matched up to the actual yield power output. Once WT and PV systems reach maximum power, MPPT techniques consider it an issue, then they find the voltage VMP (maximum voltage) and current IMP (maximum current) and naturally, within a given temperature, PV exhibit ought to receive the maximum power (MP) PMP. Wind farms with double-fed induction generators (DFIGs) can benefit from an advanced P&O algorithm that can discover the optimal DC voltage and current and track the maximum power point. Using MPPT, the maximum power of the hybrid (PV–WT–FC) system is extracted and transferred to the load in this article. A DC/DC converter's job is to get the most power out of the modules and provide it to the load. For example, a DC/DC converter is used to connect a module to the load. In order to transmit the maximum amount of power, the source's load impedance is changed and matched to the source's peak impedance at the time of peak power transfer. To keep the module working at its maximum power point, MPPT procedures are required.

Polymer electrolyte reaction kinetics and electro-osmotic drag are expressed using this method. The five equations for this FC model are represented in vector form in the following equations: Equivalent circuit for solar cells shown in Figure 2. 2021's Energies, 14, multiplied by 4 Equivalent circuit for solar cells shown in Figure 2. Figure 3: P–V and I–V Solar cell characteristics for different irradiances at a constant temperature of 25°C. Mathematical model 2.2.2. FCFuelcell components include a Proton exchange membrane, anode and cathode current collectors, and anode and cathode gas channels. Proton-exchange membrane fuel cells are depicted in Figure 4. (PEMFC). The 2.2.1 model FC's basic model comprises equations for mass, thermal energy, velocity, organisms, and charge. Five equations form the basis of this FC model. Polymer electrolyte reaction kinetics and drag are expressed by combining these equations into an electrochemical process. The five equations for this FC model are represented in vector form in the following equations: Fig. 3. P–V and I–V asymmetry Solar cell characteristics for different irradiances at a constant temperature of 25 °C. The number 2.2.F

The Equation of Continuity Carbon fibre or carbon cloth is used to make the electrodes in the FC. There is an even distribution of the reactants across the CL, and the electrodes are held in place by a porous material. Equation (4) provides the continuity equation for porosity using electrodes(5).

$$\left( \frac{\partial s\rho}{\partial t} \right) + \nabla x(\varepsilon\rho U) = 0 \quad (12)$$

This equation expresses the relationship between an object's dimensionality and its porosity.

#### Keeping the Current Pace

In Equation (6), the Navier–Stokes equation for a Newtonian fluid is provided.

$$\left( \frac{\partial(\rho U)}{\partial t} \right) + \nabla \cdot (\epsilon \rho U^2) = -\epsilon \nabla p + \epsilon F + \nabla \cdot (\epsilon \tau) - \frac{s^2 \mu U}{k} \quad (13)$$

In this equation,  $p$  is the pressure, and  $\tau$  is the stress tensor, and  $F$  is the floating mass vector, and  $s$  is the viscosity degree of the liquid. Charge Equation Conversion Electrochemical reactions are carried out using PEMFC in CL. There are two charge equations in the FC: the removal of electrons from the conductive solid phase and the transfer of protons from the membrane. Catalyst oxygen diffusion flux (ODF) and current density (CD) are utilized to compute the CL flow rate. Fig 5 Two-dimensional Poisson's equation for CL

$$\nabla \cdot i = 0 \quad (14)$$

For the loss function, we define the Jacobian matrix as that which contains the errors' derivatives with respect to each parameter.

#### IV. Artificial Neural Network Levenberg-Marquardt algorithm

To use the Levenberg-Marquardt algorithm, you need a loss function that is a sum of square errors. Hessian matrices aren't necessary for this algorithm to work. A Jacobian matrix is used instead of a gradient vector for this.

$$J_{ij} = \frac{\partial e_i}{\partial w_j} \quad (19)$$

for  $i=1, \dots, m$  and  $j=1, \dots, n$ .

Neural networks are constructed with  $n$  parameters (number of samples) and  $m$  parameters (number of samples). The Jacobian matrix has a size of  $m \times n$ .

It's possible to calculate the gradient vector of the loss function by using the following method:  
 $\nabla f = 2J^T \cdot e \quad (20)$

For example, consider a loss function that is a sum of squared errors

Hessian positivity is ensured by the damping factor, and identity is represented by the identity matrices  $I$ .  
 $H_f \approx 2J^T \cdot J + \lambda I \quad (21)$

The following equation explains how the Levenberg-Marquardt algorithm improves parameters.

$$w^{(i+1)} = w^{(i)} - (J^{(i)T} \cdot J^i + \lambda^{(i)} I)^{-1} \cdot (2J^{(i)T} \cdot e^{(i)}) \quad (22)$$

for  $i=0, 1, \dots$

In this case, Newton's technique is used using the approximation Hessian matrix when it is zero. A small training rate can be achieved by using gradient descent with a high.

The starting value of the parameter is large so that the first updates in the gradient descent direction are short steps. If each iteration fails, a certain factor is added to. The Levenberg-Marquardt algorithm approaches Newton's method as the loss diminishes. This method is often used to reduce the time it takes for the convergence to occur.

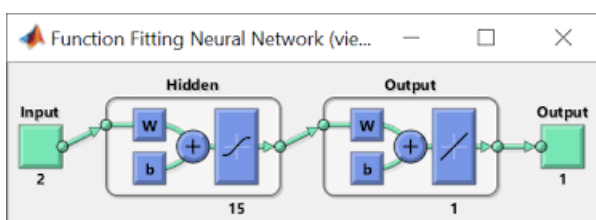


Fig 5 ANN structure.

The following diagram depicts the training of a neural network using the Levenberg-Marquardt method. The loss, the gradient, and the Hessian approximation are all calculated in the first step. Adjusting the damping parameter at each repetition reduces loss. According to the Levenberg-Marquardt algorithm, sum-of-squared-error functions can be computed using this method. When training neural networks based on those kinds of errors, it is extremely rapid.

This algorithm, however, has certain flaws. A root mean squared error or a cross-entropy error cannot be minimised by this method in the first place. Big data sets and neural networks necessitate a large Jacobian matrix, which requires a lot of memory. If our datasets or neural networks are large, we should not use the Levenberg-Marquardt algorithm.

## V. RESULTS & DISCUSSION

A MATLAB/Simulink simulation analysis is performed to determine the resistive load's maximum power output. The simulation and evaluation of a hybrid renewable energy system has been completed. Here are the MATLAB/Simulink simulation results for calculating the output power for various conventional sources after the booster has been turned on, utilising MPPT based on fuzzy logic controllers and ANNs. ANN based MPPT gives better results compared to fuzzy controller.

### 35 ohms R load after the MPPT technique.

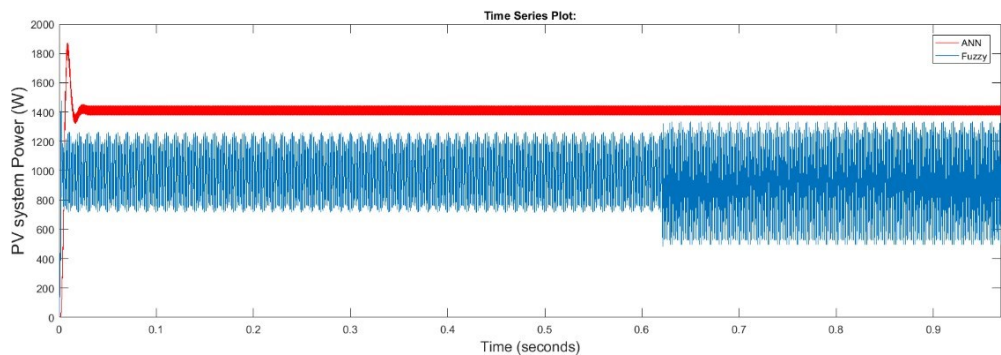


Fig6. PV system power(W) with the Fuzzy and ANN controllers

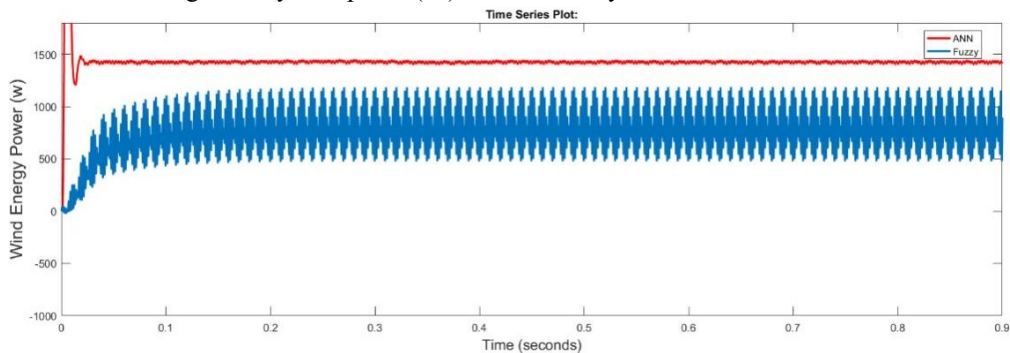


Fig7. Wind Energy power(W) with the Fuzzy and ANN controllers

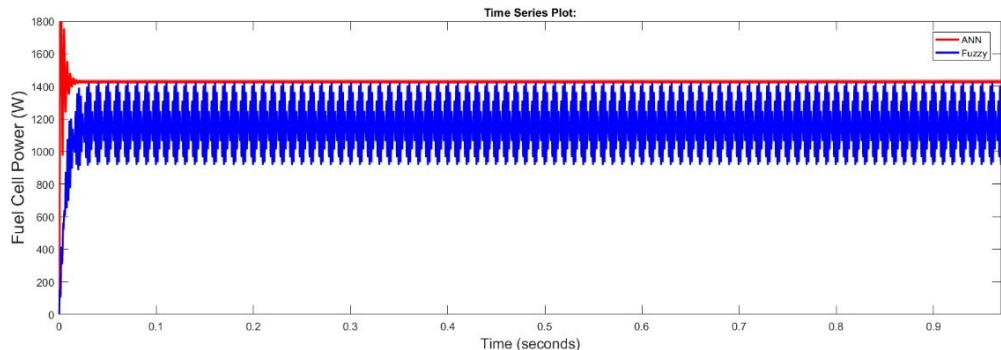


Fig8. Fuel cell power(W) with the Fuzzy and ANN controllers

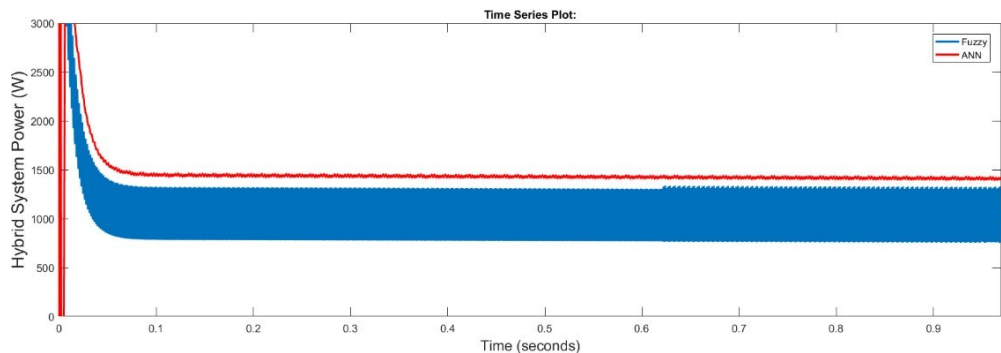


Fig9. Hybrid System power(W) with the Fuzzy and ANN controllers

From the above figures the powers of the various energy sources are given as Fuel Cell, Hybrid system, PV system and the Wind energy powers are shown in the above figures.

## CONCLUSIONS & FUTURE SCOPE

The power fluctuation has been smoothed using a control method performed using an ANN controller. A New MPPT for solar PV, wind turbine (WT), AND fuel cell (FC) systems are described in this paper. This MPPT is capable of providing rapid and accurate results in a hybrid system. As part of the case study, many random-generated scenarios were used to compute some quality indices that can be used to compare different neural network architectures. This study's findings also show that the approach is very difficult to changes the PV system's parameter values. The results suggest that the proposed hybrid system is more efficient when using the MPPT technique. The proposed hybrid system provides more power in PV, WT, and FC systems at different loads, according to the analysis. However, ANN gives better results compared to the Fuzzy controller and smoothing of the DC power. This research can be used for both a stand-alone system and grid. Future, next steps could include conducting experimental tests of the proposed MPPT in order to determine whether hardware options are more cost-effective. Research could focus on the trade-off between implementation costs and energy losses.

## REFERENCES

- [1] Esram T, Chapman PL. Comparison of photovoltaic array maximum power point tracking techniques. *IEEE Trans Energy Convers* 2007;22(2):439–49.
- [2] De Brito MAG, Galotto L, Sampaio LP, de Azevedo e Melo G, Canesin CA. Evaluation of the main MPPT techniques for photovoltaic applications. *IEEE Trans Indus Electr* 2013;60(3):1156–67.
- [3] Wang C, Nehrir MH (2008) Power Management of a StandAlone Wind/PV/Fuel Cell Energy System. *IEEE Energy Convers* 23(3):957–967
- [4] Ahmed NA, Miyatake M, Al-Othman AK (2008) Power Fluctuations Suppression of Stand-Alone Hybrid Generation Combining Solar Photovoltaic/Wind Turbine and Fuel Cell Systems. *Energy Convers Manag* 49(10):2711–2719

- [5] Onar OC, Uzunoglu M, Alam MS (2008) Modeling, control and simulation of an autonomous WT/PV/FC/Ultra-capacitor hybrid power system. *J Power Sour* 185(2):1273–1283
- [6] Wang P, Billinton R (2001) Reliability benefit analysis of adding WTG to a distribution system. *IEEE Trans Energy Convers* 16(2):134–139
- [7] Ozgener O (2006) A small wind turbine system (SWTS) application and its performance analysis. *Energy Convers Manag* 47(11):1326–1337
- [8] Gao L, Dougal R, Liu S et al (2009) Parallel-connected solar PV system to address partial and
- [9] rapidly fluctuating shadow conditions. *IEEE Trans Industr Electron* 56(5):1548–1556
- [10] Flores P, Dixon J, Ortúzar M et al (2009) Static var compensator and active power filter with power injection capability, using 27-level inverters and photovoltaic cells. *IEEE Trans Industr Electron* 56(1):130–138
- [11] Lo YK, Lee TP, Wu KH (2008) Grid-connected photovoltaic system with power factor correction. *IEEE Trans Industr Electron* 55(5):2224–2227
- [12] Patel H, Agarwal V (2008) Maximum power point tracking scheme for PV systems operating under partially shaded conditions. *IEEE Trans Industr Electron* 55(4):1689–1698
- [13] Jiang JA, Huang TL, Hsiao YT et al (2005) Maximum power tracking for photovoltaic power systems. *Tamkang J Sci Eng* 8(2):147–153
- [14] Hussein KH, Muta I, Hoshino T et al (1995) Maximum photovoltaic power tracking: an algorithm for rapidly changing atmospheric conditions. *IEEE Proc Gener Transm Distrib* 142(1):59–64
- [15] Wasynezuk O (1983) Dynamic behaviour of a class of photovoltaic power systems. *IEEE Trans Power Appar Syst* 9:3031–3037
- [16] Femia N, Granozio D, Petrone S, Spagnuolo G, Vittelli M. Predictive&adaptive MPPT perturb and observe method. *IEEE Trans Aerosp Electron Syst* 2007;43(3):934–50.
- [17] Casadei D, Grandi G, Rossi C. Single-phase single-stage photovoltaic generation system based on a ripple correlation control maximum power point tracking. *IEEE Trans Energy Convers* 2006;21(2):562–8.
- [18] Abdelsalam AK, Massoud AM, Ahmed S, Enjeti P. High-performance adaptive perturb and observe MPPT technique for photovoltaic-based microgrids. *IEEE Trans Power Electron* 2011;26(4):1010–21.